The Infrared Imaging Spectrograph (IRIS) for TMT: photometric characterization of anisoplanatic PSFs and testing of PSF-Reconstruction via AIROPA

N. Rundquist[1], S. A. Wright[1], M.Schoeck[5], A. Surya[1], J. Lu[7], P. Turri[8], E. L. Chapin[4], E. Chisholm[5] , T. Do[2], J. Dunn[4] , A. Ghez[2], Y. Hayano[6], C. Johnson[2], J. E. Larkin[2], R. L. Riddle[3], J. M. Sohn[2], R. Suzuki[6], G. Walth[1], A. Zonca[1]

1: UC San Diego, 2: UCLA, 3: Caltech, 4: NRC-HIA, 5: TMT, 6: NAOJ, 7: UC Berkeley, 8: University of British Columbia

E-mail: ***nrundqui@physics.ucsd.edu***

[11447-373]

Introduction: The InfraRed Imaging Spectrograph (IRIS) is a first-light instrument for the Thirty Meter Telescope (TMT) that will be used to sample the corrected adaptive optics field by the Narrow-Field Infrared Adaptive Optics System (NFIRAOS) with a near-infrared (0.8 - 2.4 μm) imaging camera and integral field spectrograph. To better understand IRIS science specifications we use the IRIS data simulator to characterize relative photometric precision and accuracy across the IRIS imaging camera 34"x34"field of view. Because the Point Spread Function (PSF) varies due to the effects of anisoplanatism, we use the Anisoplanatic and Instrumental Reconstruction of Off-axis PSFs for AO (AIROPA) software package to conduct photometric measurements on simulated frames using PSF-fitting as the PSF varies in single-source, binary, and crowded field use cases. We report photometric performance of the imaging camera as a function of the instrumental noise properties including dark current and read noise. Using the same methods, we conduct comparisons of photometric performance with reconstructed PSFs, in order to test the veracity of the current PSF-Reconstruction algorithms for IRIS/TMT.

Simulation Methods

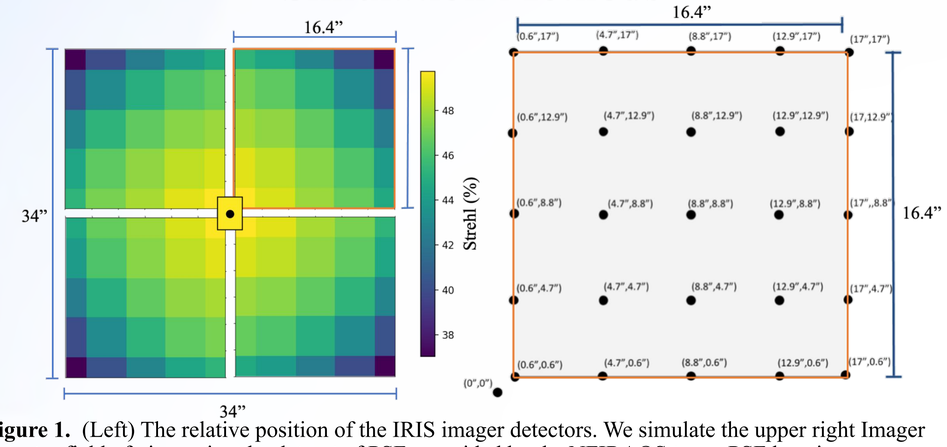

Figure 1. (Left) The relative position of the IRIS imager detectors. We simulate the upper right Imager detector field of view using the dataset of PSFs provided by the NFIRAOS team. PSF locations are on-axis (0", 0"), and a 5x5 grid over the imager field of view (right).

We use the IRIS data simulator in order to simulate point sources across the imager field of view and apply PSF-fitting and aperture photometry to sample the value distribution of sources and thereby compute photometric error for each simulated source in the field of view. We use AIROPA for PSF-fitting photometry to account for the spatially dependent PSF shown in Figure 1 (right). We compute both absolute photometric error and relative photometric precision using equations (1) and (2), respectively.

$$(1)\ Absolute\ Error\ (\%) = \frac{\bar{F} - Fse_{eded}}{F_{Seeded}} * 100 \quad (2)\ Relative\ Precision\ (\%) = \frac{\sigma_{Flux}}{\bar{F}} * 100$$

Where $\bar{F}$ is the average flux over the simulation seeds, F_{seeded} is the individual source flux for a given seed, and σ_{Flux} is the standard deviation of source flux over simulation seeds. Figure 2 depicts the confidence with which we characterize the error distribution as a function of the number of seeds used in our Monte Carlo simulations. We show the dependence of error on number of simulation seeds in Figure 2, and in order to be certain in the error values we report, we spawn 2000 seeds for each simulation case.

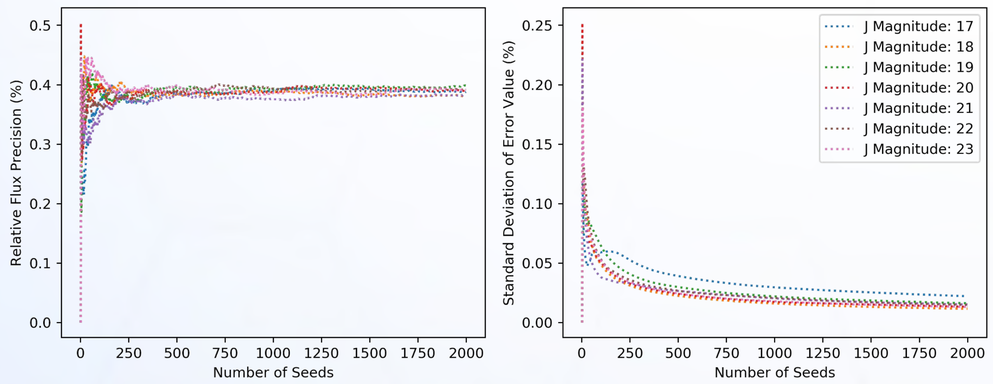

Figure 2. Relative photometric error for single star observations in J (1.24 μm) filter imaging as it changes across simulation seeds.

SNR	Magnitude (Vega)	Bandpass Integration Time (Total Seconds)				
		Z λ_c:0.87μm	Y λ_c:1.01μm	J λ_c:1.24μm	H λ_c:1.62μm	K λ_c:2.19μm
100	20	36.2	32.2	26.0	38.6	85.8
	21	91.5	82.2	67.5	120.9	263.7
	22	234.2	214.2	182.8	454.3	965.9
	23	615.7	587.6	543.6	2092.1	4340.9
	24	1719.4	1787.8	1897.7	11254.6	22985.4

Table 1. Integration times used for simulations. Magnitudes refer to source simulated, primary source magnitude, and mean source brightness for the single-star and grid, binary source case, and crowded field cases respectively. All simulations were conducted with a zenith angle of 30° and atmospheric quality of best 75%. Integration time for the Galactic Center case was 2.2 seconds, the presumed minimum.

Simulated Fields & Results

Using AIROPA and aperture photometry we characterize the photometric error in a variety of field configurations.

Single-Star and Instrumental Noise Simulations

We simulate a single star at the center of the Imager field of view and calculate photometric error across bandpasses and magnitudes. We also altered read noise and dark current values and found no effect on the results.

Magnitude (Vega)	Filter	AIROPA Error (%)	Aperture Error (%)	Strehl Ratio	PSF FWHM (pixels)	Aperture Radius (Pixels)
20	Z	0.47	0.31	0.04	2.26	8.46
	Y	0.47	0.34	0.08	2.26	8.46
	J	0.39	0.36	0.17	2.99	9.59
	H	0.35	0.61	0.32	3.91	10.72
	K	0.25	0.4	0.47	4.22	10.72
24	Z	0.5	0.38	0.04	2.26	8.46
	Y	0.51	0.82	0.08	2.26	8.46
	J	0.43	0.95	0.17	2.76	9.59
	H	0.4	1	0.32	3.91	10.72
	K	0.31	0.54	0.47	4.22	10.72

Grid-Source Photometry

We simulate a single star at each PSF location shown in Figure 1. This results in an error heat map as each source has a corresponding error value associated. Results shown in Figure 3.

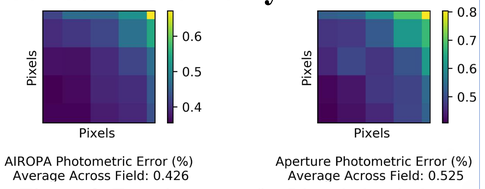

Figure 3. Error heat map for J-band simulations of point sources at each PSF location.

Binary-Source Photometry

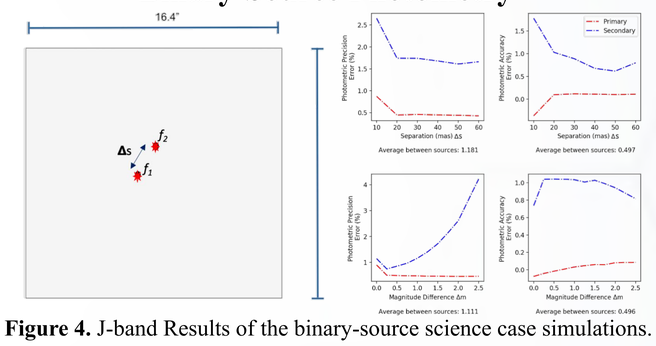

Figure 4. J-band Results of the binary-source science case simulations.

For the binary case we simulate stars at varying separations and magnitude differences. A primary magnitude of $m_J = 20$ was used, and secondary magnitude was varied by values of $\Delta m = 0.25$. We also use reconstructed PSFs in comparison with these results and assess PSF reconstruction error at ~1%.

Crowded Field Photometry

We define the crowded field configuration as a uniform distribution of star magnitudes 20 -24, distributed evenly across the field, with a minimum distance equal to 3*FWHM of the PSF (8.1 pixels for J) in order to avoid the effects of source confusion. We conduct aperture photometry for comparison. In Figure 6 all sources are colored according to their distance from the on-axis point (0", 0") of the Imager, in order to illustrate anisoplanatism in Figure 7.

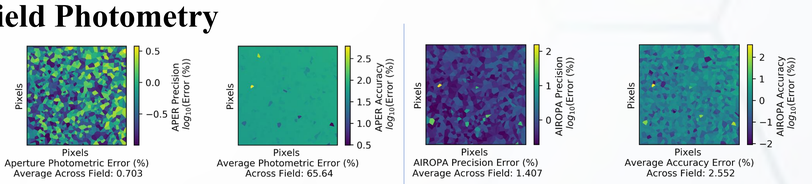

Figure 5. Aperture (left) and AIROPA (right) photometric error results across the imager field of view for the crowded field case. We adopt ~2.6% as the achieved error.

Confusion Analysis

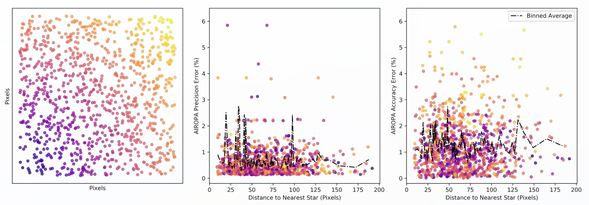

Figure 6. We assess the contributions of confusion to photometric error. We plot the relative precision (middle) and accuracy (right) of the crowded field configuration (left) as a function of each source's distance to its nearest star and find no increase in error as distance decreases.

Anisoplanatic Effect

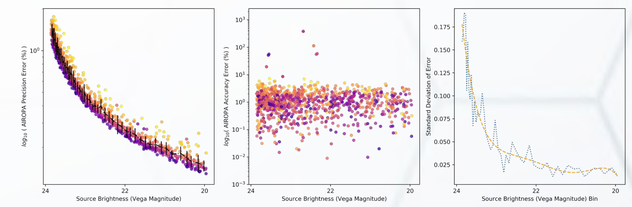

Figure 7. We assess the contributions of anisoplanatism (spatial variance of atmospheric effects) to photometric error. From the standard deviation (right) of relative precision binned by magnitude (left), we assess the effect of anisoplanatism on photometric error to be 0.025%.

Galactic Center Science Case

We simulated the Galactic Center in K, planting known sources down to 23rd magnitude and random sources down to 27th magnitude randomly distributed. We simulated 130200 sources, which is an underestimate of the actual number expected to be observed following the advent of 30-meter-class telescopes. We found the processing of the simulated frames to be highly dependent on the PSF-fitting requirements to AIROPA. Using PSF-fitting correlation values of 0.8, 0.7, 0.6, and 0.5 we achieved a source recovery of 3.4%, 6.6%, 9.7%, and 12.6% respectively as shown in Figure 8 (right). We conclude that in order to practically and accurately recover sources in such dense stellar fields, future improvements in PSF-fitting algorithms will be required.

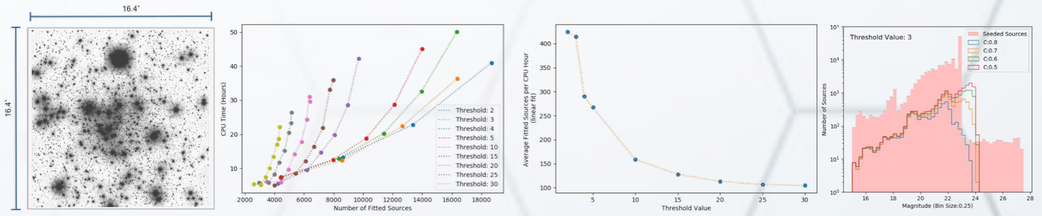

Figure 8. Results of the Galactic Center simulation, demonstrating the dependence between processing time, PSF-correlation requirements, threshold-above-noise requirements, and source recovery.

Conclusion: We conducted simulations to calculate photometric error for a variety of field configurations and assess the achievable photometric accuracy of the IRIS imager to be ~2.6%. We assess the contributions of reconstructed PSFs and anisoplanatism to photometric error to be ~1%, and 0.025% respectively. We simulated the Galactic Center and found that improvements to current PSF-fitting algorithms will be required for the practical and accurate processing of such extremely dense stellar fields.

References: 1. Larkin, J. E. et al, *SPIE* (July 2018). 2. Larkin, J. E. et al *SPIE* (August 2016). 3. Moore, A. M. et al, *SPIE* (August 2014). 4. Larkin, J. E. et al, *SPIE* (July 2010). 5. Phillips, A. C. et al, *SPIE* (August 2016). 6. Phillips, A. C. et al, *SPIE* (July 2010). 7. Wright, S. A. et al, *SPIE* (July 2016). 8. Wright, S. A. et al, *SPIE* (July 2014). 9. Wright, S. A. et al, *SPIE* (July 2010). 10. Yelda, S. et al, *Third AU4ELT Conference* (December 2013). 11. Witzel, G. et al, *SPIE* (September 2016). 12. Ciurlo, A. et al, *SPIE* (July 2018). 13. Do, T et al, *White Paper* (March 2019).